

# Rhizobial Infection Is Associated with the Development of Peripheral Vasculature in Nodules of *Medicago truncatula*<sup>1[W][OA]</sup>

Dian Guan, Nicola Stacey, Chengwu Liu, Jiangqi Wen, Kirankumar S. Mysore, Ivone Torres-Jerez, Tatiana Vernié, Million Tadege, Chuanen Zhou, Zeng-yu Wang, Michael K. Udvardi, Giles E.D. Oldroyd, and Jeremy D. Murray\*

Department of Cell and Developmental Biology, John Innes Centre, Norwich NR4 7UH, United Kingdom (D.G., N.S., C.L., T.V., G.E.D.O., J.D.M.); Samuel Roberts Noble Foundation, Ardmore, Oklahoma 73401 (J.W., K.S.M., I.T.-J., C.Z., Z.-y.W., M.K.U.); and Department of Plant and Soil Sciences, Oklahoma State University, Stillwater, Oklahoma 74078 (M.T.)

Nodulation in legumes involves the coordination of epidermal infection by rhizobia with cell divisions in the underlying cortex. During nodulation, rhizobia are entrapped within curled root hairs to form an infection pocket. Transcellular tubes called infection threads then develop from the pocket and become colonized by rhizobia. The infection thread grows toward the developing nodule primordia and rhizobia are taken up into the nodule cells, where they eventually fix nitrogen. The epidermal and cortical developmental programs are synchronized by a yet-to-be-identified signal that is transmitted from the outer to the inner cell layers of the root. Using a new allele of the *Medicago truncatula* mutant *Lumpy Infections*, *lin-4*, which forms normal infection pockets but cannot initiate infection threads, we show that infection thread initiation is required for normal nodule development. *lin-4* forms nodules with centrally located vascular bundles similar to that found in lateral roots rather than the peripheral vasculature characteristic of legume nodules. The same phenomenon was observed in *M. truncatula* plants inoculated with the *Sinorhizobium meliloti* *exoY* mutant, and the *M. truncatula* *vapyrin-2* mutant, all cases where infections arrest. Nodules on *lin-4* have reduced expression of the nodule meristem marker *MtCRE1* and do not express root-tip markers. In addition, these mutant nodules have altered patterns of gene expression for the cytokinin and auxin markers *CRE1* and *DR5*. Our work highlights the coordinating role that bacterial infection exerts on the developing nodule and allows us to draw comparisons with primitive actinorhizal nodules and rhizobia-induced nodules on the nonlegume *Parasponia andersonii*.

Legumes form an endosymbiosis with nitrogen-fixing bacteria called rhizobia in a carefully orchestrated developmental process called nodulation, which involves the infection of the epidermal cell layer and divisions of underlying cortical cells to form a new organ called a nodule. During nodulation, the bacteria enter the plant roots through special structures called infection threads, which provide access to the inner cell layers, a process that is tightly controlled by the host. In most legumes, including *Medicago truncatula*, infection threads originate from a so-called infection pocket, a structure formed by

the curling of root hairs at their tip, which serves to entrap the rhizobia. Infection threads then form as invaginations of the cell membrane and cell wall from the infection pocket and extend down through the root hair cell and eventually into the cortical layers, where the bacteria enter redifferentiated cells of the nodule (Murray, 2011). Here they are taken up into organelle-like structures called symbiosomes, where they differentiate and eventually fix nitrogen. As epidermal infection takes place, the inner cell divisions of the nodule have already started. Legume nodules can be either indeterminate, such as those found in *M. truncatula*, having a persistent apical meristem, or determinate, such as those found in *Lotus japonicus*, in which no focal meristem is evident. In *M. truncatula*, the nodule meristem takes several days to form (Timmers et al., 1999) and is subtended by a zone containing infection threads, where bacteria are released into still-developing nodule cells, followed by the nitrogen-fixing zone, which is a core of enlarged cortical cells containing the symbiosomes (Oldroyd and Downie, 2008; Oldroyd et al., 2011). The nodule also has two or more peripheral vascular bundles that converge toward the nodule apex and serve in the exchange of nutrients between roots and nodules.

The events in nodulation are initiated by lipochitooligosaccharides called Nod(ulation) factors (NF) that are produced by the rhizobia. NFs are perceived by the

<sup>1</sup> This work was supported by the Biotechnology and Biological Sciences Research Council (grant nos. CA403A13B [David Phillips Fellowship] and BB/J004553/1), the Samuel Roberts Noble Foundation, the National Science Foundation, the European Foundation (Marie Curie Intra-European Fellowship grant no. 255467 to T.V.), and the John Innes Foundation (to D.G.).

\* Corresponding author; e-mail jeremy.murray@jic.ac.uk.

The author responsible for distribution of materials integral to the findings presented in this article in accordance with the policy described in the Instructions for Authors ([www.plantphysiol.org](http://www.plantphysiol.org)) is: Jeremy D. Murray (jeremy.murray@jic.ac.uk).

<sup>[W]</sup> The online version of this article contains Web-only data.

<sup>[OA]</sup> Open Access articles can be viewed online without a subscription.

[www.plantphysiol.org/cgi/doi/10.1104/pp.113.215111](http://www.plantphysiol.org/cgi/doi/10.1104/pp.113.215111)

plant, probably by members of the LysM receptor-like kinase family LYK3 and *Nod Factor Perception (NFP)*; Amor et al., 2003; Limpens et al., 2003; Arrighi et al., 2006), and the signal is transduced by the common symbiosis pathway, which is shared with the arbuscular mycorrhizal symbiosis (Oldroyd and Downie, 2008; Oldroyd et al., 2011). The common symbiosis pathway includes CCaMK, a calcium calmodulin-dependent protein kinase (Gleason et al., 2006; Tirichine et al., 2006a), whose activation leads to the induction of transcription of several transcription factors including *Nodule Inception (NIN)*; Schauser et al., 1999; Marsh et al., 2007). *NIN* is required for both the initiation of infection threads and the initial cell divisions that lead to nodule formation, and expression of *NIN* can be induced by cytokinin (Murray et al., 2007; Plet et al., 2011). The downstream cytokinin response regulator *MtRR4* is also strongly induced during nodulation in a *Cytokinin Response1 (MtCRE1)*-dependent manner, and localizes to the early cell division center in nodule primordia and to the meristem in mature nodules (Plet et al., 2011).

The mechanism that links infection and nodule development is not known. Loss-of-function mutants such as *nin* (Schauser et al., 1999; Marsh et al., 2007) and *ccamk* (Gleason et al., 2006) that do not form infection threads invariably do not form any nodules, while mutants in which infections abort in the root hairs such as *vapyrin* (Murray et al., 2011), *lin* (Kuppusamy et al., 2004), and *rhizobium-directed polar growth (rpg)*; Arrighi et al., 2008) lead to delayed nodule development. Plant mutants such as *interacting protein of DMI3 (ipd3)*; Horváth et al., 2011; Ovchinnikova et al., 2011) and the rhizobial mutant *bacteroid development A (bacA)*; Oldroyd et al., 2011), which support normal infection thread growth but fail to form symbiosomes, have normal nodule architecture. Remarkably, in the absence of rhizobia, infection by a non-NF-producing rhizobia mutant constitutively expressing a cytokinin biosynthesis gene (Cooper and Long, 1994), and exogenous application of either NF (Truchet et al., 1991; Grosjean and Hugué, 1997) or cytokinin (Heckmann et al., 2011), constitutively active forms of the cytokinin receptor Lotus Histidine Kinase1 (LHK1)/MtCRE1 (Tirichine et al., 2007) or CCaMK (Tirichine et al., 2006; Gleason et al., 2006) can result in formation of nodule-like structures, showing that the initiation of nodule organogenesis does not require infection. However, previous studies show that rhizobial infection progression is necessary to maintain the nodule apical meristem (Voroshilova et al., 2009).

Despite the fact that mutations in several genes result in defects in both infection and organogenesis, several lines of evidence point to the genetic independence of these two programs. One line of evidence is that cortex and outer cell layers have differential responses to various species of NFs. Double *nodF/nodL* mutants that produce NFs with missing or substituted decorations are unable to induce infection threads but were still able to induce cortical cell divisions (Ardourel et al., 1994). More recently, work in *L. japonicus* showed that, in the *nod factor receptor1 (nfr1) nfr5 spontaneous nodule formation1 (snf1)*

background, no epidermal infection threads formed but transcellular infection threads in nodules occurred at a low rate with wild-type but not with *nodA* or *nodC* rhizobia (Madsen et al., 2010). Moreover, expression of gain-of-function alleles of CCaMK and LHK1 in mutants that do not support epidermal infection, such as *nfr1* or *nfr5*, can induce so-called spontaneous nodules in the absence of rhizobia (Madsen et al., 2010). Conversely, in the *hyperinfected1 (hit1)* mutant, a delay in nodule cortical cell divisions is associated with hyperinfection of the epidermis (Murray et al., 2007). While it is clear that the two programs are genetically separable, infection and organogenesis appear to be interdependent once the nodule is established, as rhizobial infection is needed for nodule apical meristem formation (Yang et al., 1992; Voroshilova et al., 2009).

Using plant and rhizobial mutants, we show that blockage of infection leads to the development of nodule-like structures that have centralized vasculature and that this phenomenon is associated with changes in auxin and cytokinin signaling. This work reveals that nodule development is influenced by the progression of bacterial infection and highlights the coordination that occurs between the cells accommodating rhizobia in the epidermis and outer root cortex and those cells in the inner cortex that are acquiring a nodule identity.

## RESULTS

### A Mutant That Aborts Rhizobial Infection in the Root Hair Curl

An *M. truncatula* mutant defective for infection by *Sinorhizobium meliloti* was identified as a nodulation mutant from a population of *Tnt1* transposon-tagged (ecotype R108) plants (Pislariu et al., 2012). Rhizobial infections that formed on the mutant aborted in the root hair curl, forming a normal-looking infection pocket but no infection threads (Supplemental Fig. S1). Rarely, what appeared to be very short intracellular infections formed, but they aborted almost immediately and never progressed across the root epidermis. We named the locus *Knocks but Can't Enter (KCE)*. Genetic analysis showed that the *kce* mutant phenotype is conditioned by a monogenic, recessive mutation ( $\chi^2 = 1.102$ ,  $P > 0.31$ ,  $n = 86$ ) that maps to the lower arm of chromosome 1 in the same region as the symbiotic gene *LIN*. We sequenced *LIN* in the *kce* mutant and found a G-to-A transition at position 1,740 in complementary DNA, which introduced a TGA stop codon. We therefore concluded that *kce* is an allele of *LIN* and we reassigned it as *lin-4*. When quantified at 6 and 14 d post inoculation (dpi), the *lin-4* mutant had more infection events than wild-type plants (Fig. 1C). Despite the early abortion of infections, *lin-4* developed nodules in a very slow manner; at 60 dpi some white bumps began to emerge, and by 90 dpi *lin-4* nodules were short white outgrowths, compared with wild-type nodules that were long and pink (Fig. 1, A and B). These nodules only formed on *S. meliloti*-infected plants and were associated

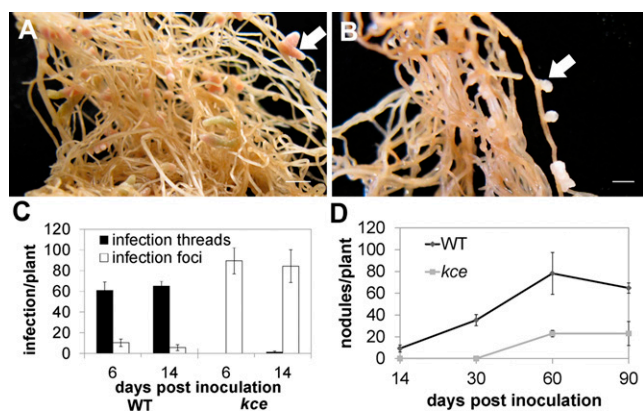


**Figure 1.** *kce* (*lin-4*) nodulation phenotype. A and B, Nodules of wild type (A) and *lin-4* (B) 80 dpi with *S. meliloti* 1021. White arrows highlight nodules. Scale bars = 5 mm. C, Mean ( $\pm$ SD) number of infection threads and infection foci of the wildtype (WT) and *lin-4* 6 and 14 dpi with *lacZ*-tagged *S. meliloti* 1021 ( $n = 5$ ). D, Mean ( $\pm$ SD) number of nodules of the wild type (WT) and *lin-4* 14, 30, 60, and 90 dpi with *S. meliloti* 1021 ( $n = 8$ ).

with aborted infections. Nodule numbers on *lin-4* were reduced at all examined time points (Fig. 1D). An acetylene reduction assay on *lin-4* nodules indicated they were deficient in nitrogen fixation (data not shown), and the plants showed signs of nitrogen deprivation (yellowing of leaves and anthocyanin accumulation in the shoot) and started to die after 3 months of growth.

#### The Infection-Induced Nodules in *lin-4* Are Centrally Vascularized

Sectioning of wild-type nodule primordium revealed that the initial cell divisions were an ordered series of

periclinal and anticlinal divisions in the cortical, endodermal, and pericycle cell layers accompanied by cell expansion that resulted in a bulge in the epidermis (Supplemental Fig. S2A). In *lin-4* primordia, early cell divisions also occurred in all three cell layers but were significantly delayed, and cell expansion was not seen at this stage (Supplemental Fig. S2B). This is identical to *lin-1* as described by Kuppusamy et al. (2004). Also, the area where the cortical cell divisions occurred was limited to a shorter interval, and the divisions were less coordinated such that the layered organization of cell layers seen in the wild type was lost (Supplemental Fig. S2). Surprisingly, as the *lin-4* nodules grew over time they developed a central vascular bundle (Fig. 2, B and D) similar to lateral roots (Fig. 2, E and F). This contrasted markedly with the wild-type nodules, where multiple vascular bundles developed at the nodule periphery (Fig. 2, A and C). However, *lin-4* nodule vascular strand organization was often different from that of the lateral roots; in particular, the *lin-4* nodules sometimes had a centrally fused xylem strand (Fig. 2D). In addition, examination of longitudinal sections revealed that the apical region of the *lin-4* nodule (Fig. 2B) lacks the characteristic organization of lateral roots (Supplemental Fig. S3). To investigate the nature of these nodules we tested marker genes for lateral roots and nodules using quantitative reverse transcription-PCR (QRT-PCR) from *lin-4* and wild-type spot-inoculated roots. We used the *M. truncatula* Gene Expression Atlas database to identify two marker genes expressed in the root tip, *Ferredoxin I* (Medtr2g006290) and a membrane protein (Medtr7g011090), which are not expressed in nodules (Holmes et al., 2008). QRT-PCR showed that *lin-4* nodules have significantly lower expression of these root tip marker genes compared with lateral roots (Fig. 3A). In addition, we tested expression of the nodulation-

#### WT

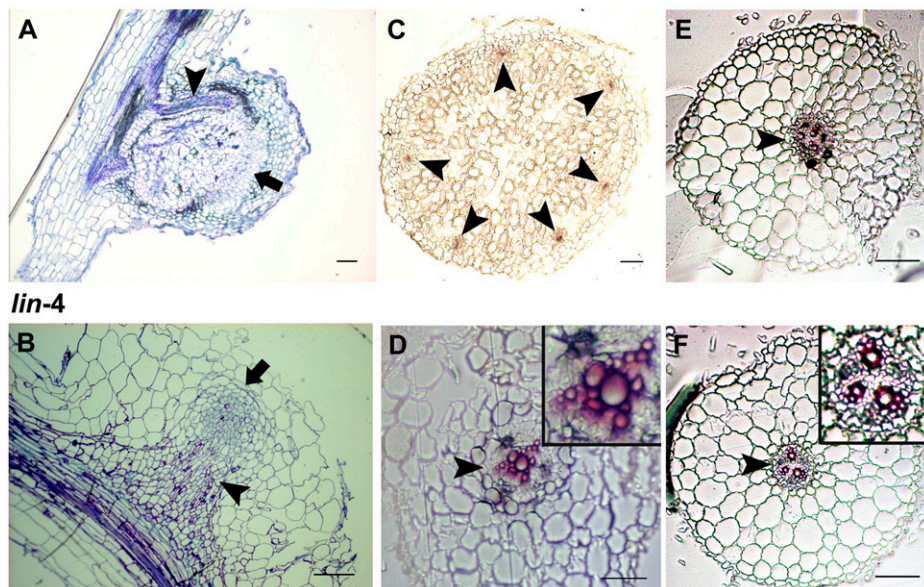


**Figure 2.** *lin-4* nodule vascular bundles are centrally localized. A to D, Longitudinal (A and B) and cross (C and D) sections of wild-type (A and C) and *lin-4* (B and D) nodules. Black arrows highlight nodule meristems, and black arrowheads highlight vascular bundles. E and F, Lateral root cross sections of the wild type (E) and *lin-4* (F). A and B are stained with toluidine blue, C to F with phloroglucinol. WT, Wild type. Scale bars = 100  $\mu$ m.

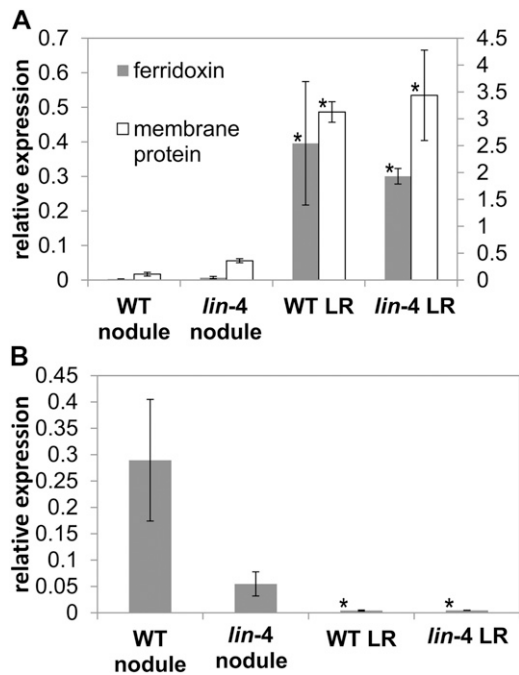


**Figure 3.** *lin-4* nodules do not express lateral root marker genes. A, Root-tip marker gene expression in wild-type and size-matched *lin-4* nodules and lateral roots measured by QRT-PCR normalized using *EF-1 $\alpha$* . Marker genes are *ferridoxin 1* (Medtr2g006290) and a plant integral membrane protein (Medtr7g011090). B, *NIN* gene expression in wild-type and *lin-4* nodules and lateral roots measured by QRT-PCR normalized using *MtEF-1 $\alpha$* . The results represent three biological replicates ( $\pm$ sd). A comparison of gene expression was made between *lin* nodules and the other tissues (Welch's *t* test, \* $P < 0.05$ ). WT, Wild type; LR, lateral roots.

specific transcription factor *NIN* (Schauer et al., 1999; Marsh et al., 2007). *NIN* gene expression was lower in *lin-4* nodules than in wild-type nodules, but this difference was not significant ( $P > 0.05$ , Student's *t* test). However, the expression of *NIN* was significantly higher in *lin-4* nodules than in the lateral roots (Fig. 3B). We also checked the expression of other nodulation marker genes in *lin-4* nodules. *ENOD20* has been shown to be induced in dividing cortical cells in nodule primordia, in cells containing infection threads, and later in nodules in the infection and nitrogen-fixing zones (Vernoud et al., 1999), whereas *HAP2.1* is reported to express in the nodule meristem (Comber et al., 2006, 2008). Relative transcript levels of *ENOD20* and *HAP2.1* in developing nodules were not significantly lower in *lin-4* than in the wild type (data not shown).

#### Early Abortion of Rhizobial Infection in the Root Hair Leads to the Development of Nodules with Central Vascular Bundles

To test whether the abnormal nodules that formed on *lin-4* were a result of the premature termination of infection or a specific feature of the *lin-4* allele, we studied

some rhizobial and plant infection mutants where rhizobial infection aborts at a similar stage. First we tested the *M. truncatula vapyrin-2* and *lin-1* mutants. These mutants have a mixture of infections that either abort within root hairs or penetrate into the nodules (Kuppusamy et al., 2004; Murray, 2011). Nodule sectioning revealed these structures were devoid of bacteria (Fig. 4A). When nodules were allowed to develop over several months, *lin-1* developed a mixture of nodules having either central or peripheral vascular bundles (Fig. 4, C and D). This contrasts with the *kce (lin-4)* phenotype, which featured only centrally vascularized nodules. This difference may be due to the differing genetic backgrounds of these alleles (*lin-1*, Jemalong A17; *lin-4*, R108). We then examined the nodules more closely to determine if there was a relationship between the stage of rhizobial infection and vasculature pattern. For the *lin-1* mutant, nodules with peripheral vasculature were almost always (95%,  $n = 20$ ) found to be associated with a greatly thickened infection thread either in the nodule epidermis or possibly in the outer cortex (Fig. 4C), while in the instances where nodules had central vascular bundles infection thread development was limited to root hairs and was not evident in nodule cross sections (Fig. 4D). This contrasted with the *lin-4* allele, in which infection threads always terminated

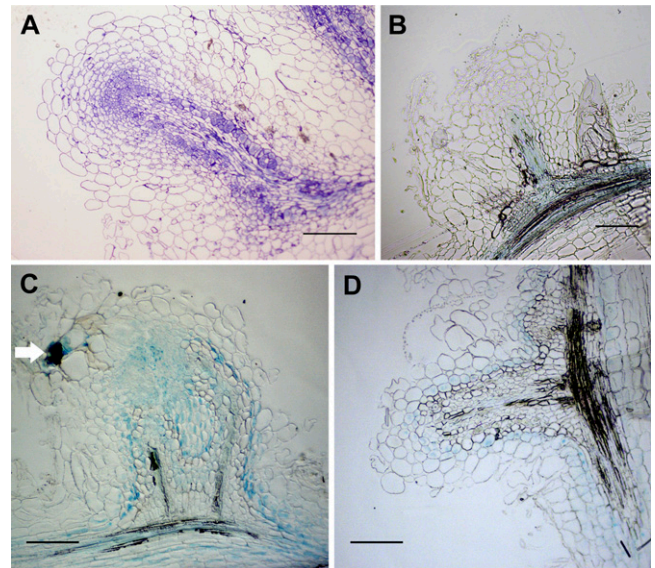


**Figure 4.** Rhizobial infections that abort in the root hair curl lead to abnormal nodule organogenesis featuring a central vascular bundle. A, A *vpy-2* nodule, stained with toluidine blue. B, An *S. meliloti* 1021 *exoY* mutant-induced nodule on the wild type (ecotype R108). C and D, *lin-1* forms two types of nodules: nodules with branched, peripheral vascular bundles (C) and nodules with central vascular bundles (D). Note the thickened infection thread in the nodule outer cortex (white arrow) in C, visualized by 5-bromo-4-chloro-3-indolyl- $\beta$ -D-galactopyranoside acid staining. Nodules were harvested at 60 dpi. Longitudinal nodule sections of 10- $\mu$ m thickness are shown. Scale bars = 200  $\mu$ m.

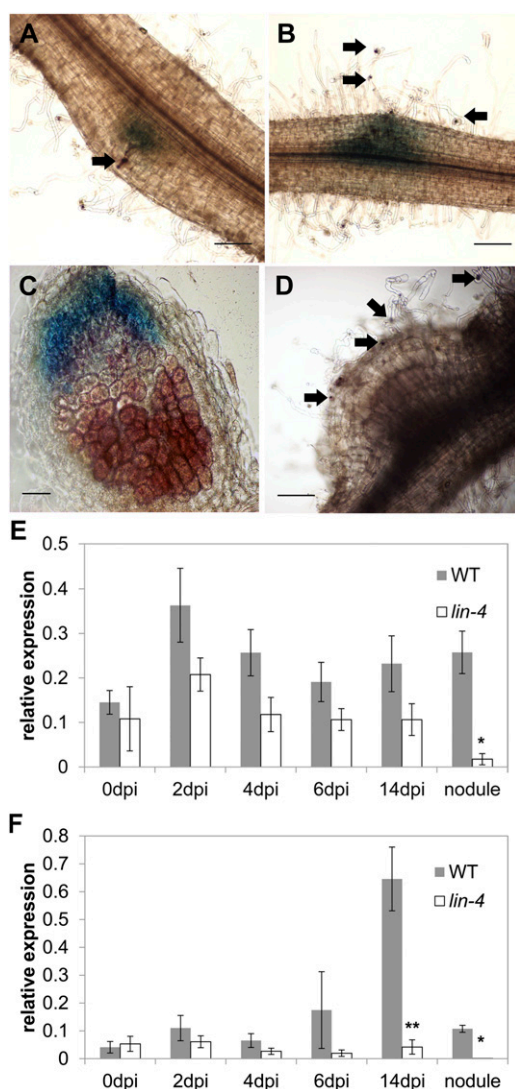


**Figure 5.** Cytokinin signaling is not maintained in *lin-4* nodule organogenesis. A–D, Wild type (A and C) and *lin-4* (B and D) transformed with *pMtCRE1::GUS* using the hairy root transformation system. A and B, 6 dpi with *S. meliloti* 1021 carrying *lacZ*. C, Wild-type nodule 13 dpi with *S. meliloti* 1021 carrying *lacZ*. D, *lin-4* nodule 45 dpi with *S. meliloti* carrying *lacZ*. 5-bromo-4-chloro-3-indolyl- $\beta$ -glucuronide was used to stain for GUS activity in A to D, seen as blue in A to C. E and F, *MtCRE1* (E) and *MtRR4* (F) gene expression in wild-type and *lin-4* spot-inoculated roots (0, 2, 4, 6, and 14 dpi) and excised size-matched nodules (see “Materials and Methods”) measured by QRT-PCR, normalized using *MtEF-1 $\alpha$* . Results represent three biological replicates ( $\pm$ sd). Expression in *lin* versus wild-type nodules was compared at the different time points (Welch’s *t* test, \* $P < 0.05$ ; \*\* $P < 0.01$ ). Infection foci and infection threads containing rhizobia were detected by LacZ activity using 5-bromo-6-chloro-3-indolyl- $\beta$ -D-galactopyranoside (indicated by black arrows). Scale bars = 200  $\mu$ m (A, B, and D) and 100  $\mu$ m (C).

in root hairs and never reached the base of the epidermal cell (Supplemental Fig. S1B). We then tested a *S. meliloti* mutant that is defective in the first step of exopolysaccharide biosynthesis, which leads to the abortion of rhizobial infection in the root hair curl

and the occasional initiation of infection threads that abort in the root hair. Vascular bundles in the small nodules produced by the *exoY* mutant also developed in a central position (Fig. 4B).

#### Cytokinin Signaling Is Not Maintained in *lin-4* Nodule Development

One of the earliest events during nodule organogenesis is cytokinin signaling. To test whether the development of centrally vascularized nodules is associated with decreased cytokinin signaling, we tested the expression of the cytokinin receptor *MtCRE1* and the type-A cytokinin response regulator *MtRR4* in *lin-4* nodules. We studied *MtCRE1* expression by using a fusion of the *MtCRE1* promoter with the  $\beta$ -glucuronidase (GUS) reporter (Lohar et al., 2006). During nodulation, cytokinin signaling is activated during early cell divisions and as the nodule develops it is strongly maintained in the nodule meristem (Lohar et al., 2006). We compared wild-type and mutant nodules of similar size, which required using relatively old nodules from the mutant. Wild-type nodules of a similar age would be senescent, but mutant nodules at this point were still growing, albeit slowly. In early development, the induction of *MtCRE1* in *lin-4* nodules was similar or slightly greater than in the wild type (Fig. 5, A and B), but in fully emerged nodules (45 dpi) *MtCRE1* gene expression was greatly reduced or absent as seen using promoter-GUS (Fig. 5, C and D) and QRT-PCR (Fig. 5E). *MtRR4* gene expression was consistently lower in *lin-4* nodules and was significantly lower when nodules of a similar developmental stage (approximately 1 mm in length) were compared (Fig. 5F).

#### *DR5::GUS* Is Expressed Ectopically in *exoY*-Induced Nodules

Because interactions between cytokinin and auxin are central to the development of vascular patterning, we used a line expressing the auxin reporter *DR5::GUS* to study the spatial distribution of auxin signaling. Wild-type nodules exhibited *GUS* expression that was mostly limited to the phloem tissue of the nodule vascular strands, with no staining in the infection zone (Fig. 6A). Inoculation using the *exoY* mutant rhizobia, which induces centrally vascularized nodules, revealed *DR5* expression in the vascular bundle and, surprisingly, in the surrounding cells (Fig. 6B). For comparison, we examined lateral roots from infected plants and found they had expression in the vascular bundle and in the epidermal cell layer, but no expression in the intervening cortical cell layers (Fig. 6C).

## DISCUSSION

### Nodule Infection Is Required for Normal Vascular Development in Nodules

We provide evidence that successful epidermal infection is required for normal nodule development during

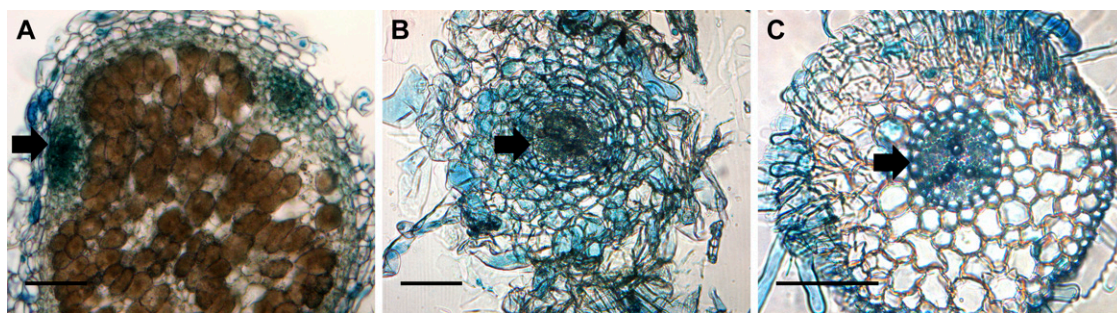


**Figure 6.** Auxin response is altered in central vascular bundle nodules. A and B, Nodules cross sections of *DR5::GUS* stable transgenic plants inoculated with wild-type *S. meliloti* 1021 10 dpi (A) or *S. meliloti* 1021 *exoY* mutant 60 dpi (B). C, Lateral root sections of *DR5::GUS* stable transgenic plants. Sections are 50  $\mu\text{m}$  thick. Black arrows highlight vascular bundles. Scale bars = 100  $\mu\text{m}$ .

nodulation in *M. truncatula*. We found that nodules that form on the *kce* (*lin-4*) mutant have a central rather than peripheral vascular bundle. This configuration is similar to lateral roots and actinorhizal nodules and the rhizobia-induced nodules that develop on the non-legume *Parasponia* spp. This outcome is independent of the plant genotype as shown by the occurrence of nodules having either central or peripheral vasculature on the same plants on certain alleles of *opy* and *lin* mutants in a manner that directly corresponds to the extent of infection progression. In addition, rhizobial *exoY* mutants that abort early in infection also produce nodules with a centrally located vascular strand. The distinct structure of these growths and analysis of marker gene expression suggests that symbiotic identity is retained despite the fact that these nodules are not colonized.

This work implies that appropriate nodule development requires the ongoing infection of bacteria, and in cases where bacterial infection is initiated but progression aborts, there is a direct impact many cell layers away in the developing nodule primordia. The fact that this impacts the final nodule structure highlights the level of control exerted by the progressing infection process on the developing cells of the nodule. Support for the idea that infection determines nodule development outcomes is provided by Hirsch et al. (1985). They showed that *Agrobacterium tumefaciens* and symbiotic deficient *Rhizobium trifolii* transconjugants carrying nodulation sequences from *S. meliloti* were able to induce nodules with peripheral vascular bundles on *Medicago sativa*, but formed nodules with central vascularization when white clover (*Trifolium repens*) roots were inoculated. When the nodules were examined it was found that despite lacking infection threads the nodules formed on *M. sativa* contained large pockets of intracellular bacteria, while the nodules on the white clover roots were not colonized. Although our experiments were limited to *M. truncatula*, nodules with central vascular tissue were reported for soybean (*Glycine max*) infected by a *Bradyrhizobium japonicum* mutant that lacked the high  $M_r$  lipopolysaccharide I. These nodules also lacked bacteria (Stacey et al., 1991). The *L. japonicus aberrant localization of bacteria inside nodule1* mutant appears to

develop central vasculature in uncolonized nodules, which may suggest this phenomenon is widespread in legumes (Imaizumi-Anraku et al., 2000).

#### A Role for Auxin and Cytokinin in Infection-Dependent Nodule Development Outcomes

How might infection affect development in such a striking manner? There are several interesting exceptions to the link between infection and the development of peripheral vascular bundles that provide important clues to the mechanisms underlying this phenomenon. First, nodules induced by NFs alone can sometimes have normal positioning of the vascular strands (Truchet et al., 1991; Grosjean and Huguet, 1997). Also, application of either exogenous cytokinin or the *L. japonicus snf2* mutant with constitutively active cytokinin signaling produces nodules with peripheral vascular bundles in the absence of infection (Tirichine et al., 2006b; Heckmann et al., 2011). Similarly, the *snf1* mutant also produces spontaneous nodules with normal architecture (Tirichine et al., 2006b). Therefore, it appears that the requirement for infection can be obviated by activation of downstream processes, in particular cytokinin signaling. Counter to this, auxin transport inhibitors like naphthylphthalamic acid induce nodules that lack vascular strands altogether (Hirsch et al., 1989; Van De Wiel et al., 1990; Takashi et al., 2011) or nodules with centrally proliferating vascular tissue (Wu et al., 1996; Rightmyer and Long, 2011), underscoring the central role of polar auxin transport in vascular bundle formation. NFs applied to legume roots have a dramatic effect on polar auxin transport (Mathesius et al., 1998; Boot et al., 1999). Spot application of NFs or rhizobia on white clover roots has been shown to induce a strong local repression of expression from the promoter of the auxin reporter gene *GH3* (Mathesius et al., 1998). It is not known how this effect is exerted, but cytokinin perception has been shown to be required for the rhizobia-induced changes in auxin transport that occur during nodulation (Plet et al., 2011), and flavonoids, which are essential for nodulation, also exert effects on auxin transport (Wasson et al., 2006; Subramanian et al.,

2007; Zhang et al., 2009). We propose that the advancing infection thread results in local signaling outputs, most likely in response to NF, which mediate appropriate cytokinin and auxin distribution in the developing nodule primordia.

NFs are produced by rhizobia enclosed in infection threads within the nodule (Marie et al., 1992) and these are likely to initiate the coordination of nodule development with infection progression. While NF-induced nuclear calcium oscillations accompany the advance of infection through the underlying cortical cell layers (Sieberer et al., 2012), NF signaling remains restricted to those cells in close contact with the invading rhizobia. Thus, NF signaling alone may not be sufficient to explain the coordination of infection and nodule development that are separated by multiple cell layers. NF perception may activate a transcellular signal that drives developmental changes in the inner root cortex, and such signaling must be maintained to ensure appropriate nodule development. It is possible that the production of NFs within the center of the nodule results in changes in cytokinin and auxin distribution that have developmental consequences. Auxin has a well-established role in vascular differentiation, and xylem formation in particular is associated with high levels of auxin stimulation in the presence of cytokinin (Aloni et al., 2006). This idea is consistent with the observation that expression of the auxin reporter *GH3* is initially uniform within nodules prior to infection, but as the nodule develops, *GH3* expression becomes diminished at the center of the nodule where infection occurs and is limited to the nodule periphery and is especially high in the vascular bundles (Mathesius et al., 1998; Pacios-Bras et al., 2003; Takanashi et al., 2011). We find that marker genes for cytokinin and auxin signaling are deregulated when infection is prematurely aborted. Because cytokinin can induce normal nodules while auxin cannot, it seems most likely that the abnormal nodule development is ultimately a result of altered cytokinin signaling. However, auxin can directly repress cytokinin at the biosynthesis and signaling levels (Cheng et al., 2013; Zhao et al., 2010), so it remains possible that ectopic auxin signaling leads to the repression of cytokinin, which in turn leads to abnormal vascular development.

### Implications for Nodule Evolution

Nodules with central vascular bundles result from rhizobial infection of members of the nonlegume genus *Parasponia* (Trinick, 1979; Lancelle and Torrey, 1985). The infection program in *Parasponia* spp. does not utilize root hairs; infection threads are formed only after penetration of the bacteria into the root cortex, which leads to the formation of a small non-vascularized pre-nodule near to where the main centrally vascularized nodule will emerge and eventually become infected (Bender et al., 1987a, 1987b). Similarly, nodules induced by *Frankia* spp. involve the formation of a pre-nodule so that the initial epidermal

infection and lateral organ development programs are separate both temporally and spatially. It has been proposed that these independent processes present in actinorhizal nodulation have been merged together in legumes (Gualtieri and Bisseling, 2000; Laplaze et al., 2000). Our finding that physical separation of infection from the emerging nodule leads to the development of nodules with a central vascular arrangement supports this hypothesis. These findings suggest that by achieving a better understanding of the impact of infection on nodule development we will gain insights into the evolution of this legume-specific innovation in nodule architecture.

## MATERIALS AND METHODS

### Plant Materials and Bacterial Strains

Seeds of *Medicago truncatula* Jemalong A17, *lin-1*, and *M. truncatula* R108, *vapyrin-2*, and *kce (lin-4)* were scarified with concentrated sulfuric acid for about 10 min, rinsed six times, surface sterilized in 100% bleach for 2 min, rinsed six more times, then imbibed in sterile water and plated on 1% (w/v) deionized water agar plates. Seeds were left at 4°C for 1 d and germinated on inverted agar plates at 23°C overnight. For hairy root transformation, *M. truncatula* seedlings were transformed with *Agrobacterium rhizogenes* strain ARqua1 carrying the appropriate binary vector using standard protocols (Boisson-Dernier et al., 2001). For nodulation assays, either *Sinorhizobium meliloti* 1021, *S. meliloti* 1021 pXLGD4, or *S. meliloti* Rm7210 exoY210::Trn5 (Leigh et al., 1985) strain was used. The *DR5::GUS* marker line was produced by stable transformation of *M. truncatula* leaves using the *Agrobacterium tumefaciens* strain EHA105 harboring the *DR5::GUS* construct.

### Marker Gene QRT-PCR Assay

The germinated *M. truncatula* seedlings were put on buffered nodulation medium containing 0.1 μM 2-aminoethoxyvinyl-Gly (AVG) for 2 d until the main roots grew to a length of about 3 cm. The roots were spot inoculated in the differentiation zone with 1 μL of *S. meliloti* 1021 pXLGD4 culture (optical density at 600 nm ≈ 0.2). The site of inoculation was marked at the back of the plate. The inoculated section was harvested at different time points. For each time point, more than six root segments of about 1 mm in length were collected. As *kce (lin-4)* nodules emerge much slower than wild-type nodules, we attempted to account for this by isolating nodules from *kce (lin-4)* and emerging lateral roots from the wild type that were matched in size. For the size-matched samples, an emerged *lin-4* nodule (70 dpi) and a just-emerged lateral root tip, each 1 mm in length, were excised. RNA extractions and complementary DNA synthesis were carried out using the RNeasy Micro kit (Qiagen) and SuperScript II Reverse Transcriptase (Invitrogen). QRT-PCR reaction was done using LightCycler 480 SYBR Green I Master (Roche Applied Science) reagents and analyzed using LightCycler 480 Real-Time PCR System (Roche Applied Science) over 45 cycles of 95°C for 25 s, 58°C for 25 s, and 72°C for 40 s after an initial denaturation at 95°C for 2 min. The internal control gene was *MtEF-1α*. Data from three technical replicates and three biological repeats were analyzed using the comparative cycle threshold method. The *SD* values were calculated using Excel 2007 software. Primers used had PCR efficiencies greater than 90%. Means comparisons were based on relative quantity values. Primer sets used in QRT-PCR: *MtHRR4*: 5'-ATGCTTTTGTTCCGGGTTTA-3'; 5'-CTGCACCTTCTCCAAACAT-3'. *MtCRE1*: 5'-CACCACCCTTTGGCTTCTAA-3'; 5'-CACTAAGTAGCGGCTTTCG-3'. *MtGH3*: 5'-ACTTAACGGTGCACCTGACC-3'; 5'-AACTGACGACGGTCCATTTTC-3'. *MtNIN*: 5'-CAGACTACCATCAGCTGCA-3'; 5'-CCACAGTTGGTCTGGAGGT-3'. Root-specific ferridoxin: 5'-GCAACCACACCTGCTTTGTA-3'; 5'-GTGGTGGTGTGATTGACAC-3'. Root-specific membrane protein: 5'-AGGAGCAGTGTGGAATGAC-3'; 5'-TGCTGACAAAAAGCAAACCA-3'. *MtEF-1α*: 5'-ATTCCAAAGCGCGCTGCATA-3'; 5'-CTTTGCTTGGTGTGTTAGATGG-3'.

### Nodulation Assay

*M. truncatula* seedlings were grown in 40 cell trays with a Terragreen (Oil-Dri UK) and silver sand 1:1 mixture for 7 d before inoculation with rhizobia. A

24-h culture of rhizobia was spun down and resuspended in buffered nodulation medium to an optical density at 600 nm of 0.02, and 3 mL of the culture was used to inoculate each of the growing *M. truncatula* plants. Nodules and infection events were counted 6 to 90 dpi.

## GUS Staining and LacZ Staining

*pCRE1::GUS* construct was from Lohar et al. (2006). Hairy root transformation of *M. truncatula* and selection of kanamycin-resistant plants were performed as described above. Plants were transferred to a 50:50 Terra Green and silver sand mixture and inoculated with *S. meliloti* 1021 pXLGD4 as described above. GUS activity (Vernoud et al., 1999) and LacZ activity (Pichon et al., 1994) of whole roots and nodules were performed as previously described.

## Technovit Embedding, Sectioning, and Section Staining

Collected tissues were fixed in 2.5% (v/v) glutaraldehyde as described in (Vernié et al., 2008). After fixation, tissues were embedded in Technovit 7100 (Kulzer GmbH) resin according to the manufacturer's instructions and 10- $\mu$ m transverse or longitudinal sections were taken. Sections were stained with 0.5% (w/v) toluidine blue O in 0.5% (w/v) sodium tetraborate buffer or 20 mg mL<sup>-1</sup> phloroglucinol in 20% HCl (v/v) before taking pictures under a Nikon Eclipse E800 microscope.

## Supplemental Data

The following materials are available in the online version of this article.

**Supplemental Figure S1.** *kce* (*lin-4*) rhizobial infection phenotype.

**Supplemental Figure S2.** Early cell divisions in wild-type and *lin-4* longitudinal sections after *S. meliloti* 1021 inoculation.

**Supplemental Figure S3.** R108 (wild type) lateral root longitudinal section stained with toluidine blue.

## ACKNOWLEDGMENTS

We thank Kate VandenBosch for sending us the *pMtCRE1::GUS* construct, Allan Downie for critical reading of the manuscript, and Susan Bunnell for technical assistance.

Received January 30, 2013; accepted March 25, 2013; published March 27, 2013.

## LITERATURE CITED

- Aloni R, Aloni E, Langhans M, Ullrich CI (2006) Role of cytokinin and auxin in shaping root architecture: regulating vascular differentiation, lateral root initiation, root apical dominance and root gravitropism. *Ann Bot (Lond)* **97**: 883–893
- Amor BB, Shaw SL, Oldroyd GE, Maillet F, Penmetsa RV, Cook D, Long SR, Dénarié J, Gough C (2003) The *NFP* locus of *Medicago truncatula* controls an early step of Nod factor signal transduction upstream of a rapid calcium flux and root hair deformation. *Plant J* **34**: 495–506
- Ardourel M, Demont N, Debelle F, Maillet F, de Billy F, Promé JC, Dénarié J, Truchet G (1994) *Rhizobium meliloti* lipooligosaccharide nodulation factors: different structural requirements for bacterial entry into target root hair cells and induction of plant symbiotic developmental responses. *Plant Cell* **6**: 1357–1374
- Arrighi JF, Barre A, Ben Amor B, Bersoult A, Soriano LC, Mirabella R, de Carvalho-Niebel F, Journet EP, Ghérardi M, Huguet T, et al (2006) The *Medicago truncatula* lysin motif-receptor-like kinase gene family includes *NFP* and new nodule-expressed genes. *Plant Physiol* **142**: 265–279
- Arrighi JF, Godfroy O, de Billy F, Saurat O, Jauneau A, Gough C (2008) The *RPG* gene of *Medicago truncatula* controls Rhizobium-directed polar growth during infection. *Proc Natl Acad Sci USA* **105**: 9817–9822
- Bender GL, Goydych W, Rolfe B, Nayudu M (1987a) The role of Rhizobium conserved and host specific nodulation genes in the infection of the non-legume *Parasponia andersonii*. *Mol Gen Genet* **210**: 299–306
- Bender GL, Nayudu M, Goydych W, Rolfe BG (1987b) Early infection events in the nodulation of the non-legume *Parasponia andersonii* by Bradyrhizobium. *Plant Sci* **51**: 285–293
- Boisson-Dernier A, Chabaud M, Garcia F, Bécard G, Rosenberg C, Barker DG (2001) Agrobacterium rhizogenes-transformed roots of *Medicago truncatula* for the study of nitrogen-fixing and endomycorrhizal symbiotic associations. *Mol Plant Microbe Interact* **14**: 695–700
- Boot KJM, van Brussel AAN, Tak T, Spaik HP, Kijne JW (1999) Lipochitin oligosaccharides from *Rhizobium leguminosarum* bv. *viciae* reduce auxin transport capacity in *Vicia sativa* subsp. *nigra* roots. *Mol Plant Microbe Interact* **12**: 839–844
- Cheng ZJ, Wang L, Sun W, Zhang Y, Zhou C, Su YH, Li W, Sun TT, Zhao XY, Li XG, et al (2013) Pattern of auxin and cytokinin responses for shoot meristem induction results from the regulation of cytokinin biosynthesis by AUXIN RESPONSE FACTOR3. *Plant Physiol* **161**: 240–251
- Combiér JP, Frugier F, de Billy F, Boualem A, El-Yahyaoui F, Moreau S, Vernié T, Ott T, Gamas P, Crespi M, et al (2006) MtHAP2-1 is a key transcriptional regulator of symbiotic nodule development regulated by microRNA169 in *Medicago truncatula*. *Genes Dev* **20**: 3084–3088
- Combiér JP, de Billy F, Gamas P, Niebel A, Rivas S (2008) Transcription of the expression of the transcription factor MtHAP2-1 by a uORF controls root nodule development. *Genes Dev* **22**: 1549–1559
- Cooper JB, Long SR (1994) Morphogenetic rescue of *Rhizobium meliloti* nodulation mutants by trans-zeatin secretion. *Plant Cell* **6**: 215–225
- Gleason C, Chaudhuri S, Yang T, Muñoz A, Poovaiah BW, Oldroyd GED (2006) Nodulation independent of rhizobia induced by a calcium-activated kinase lacking autoinhibition. *Nature* **441**: 1149–1152
- Grosjean C, Huguet T (1997) A persistent meristem is formed in nodular structures elicited by Nod factor or by a *Rhizobium meliloti* exopolysaccharide mutant in alfalfa plants which nodulate spontaneously. *Plant Sci* **127**: 215–225
- Gualtieri G, Bisseling T (2000) The evolution of nodulation. *Plant Mol Biol* **42**: 181–194
- Heckmann AB, Sandal N, Bek AS, Madsen LH, Jurkiewicz A, Nielsen MW, Tirichine L, Stougaard J (2011) Cytokinin induction of root nodule primordia in *Lotus japonicus* is regulated by a mechanism operating in the root cortex. *Mol Plant Microbe Interact* **24**: 1385–1395
- Hirsch AM, Bhuvaneshwari TV, Torrey JG, Bisseling T (1989) Early nodulin genes are induced in alfalfa root outgrowths elicited by auxin transport inhibitors. *Proc Natl Acad Sci USA* **86**: 1244–1248
- Hirsch AM, Drake D, Jacobs TW, Long SR (1985) Nodules are induced on alfalfa roots by *Agrobacterium tumefaciens* and *Rhizobium trifolii* containing small segments of the *Rhizobium meliloti* nodulation region. *J Bacteriol* **161**: 223–230
- Holmes P, Goffard N, Weiller GF, Rolfe BG, Imin N (2008) Transcriptional profiling of *Medicago truncatula* meristematic root cells. *BMC Plant Biol* **8**: 21
- Horváth B, Yeun LH, Domonkos A, Halász G, Gobatto E, Ayaydin F, Miró K, Hirsch S, Sun J, Tadege M, et al (2011) *Medicago truncatula* IPD3 is a member of the common symbiotic signaling pathway required for rhizobial and mycorrhizal symbioses. *Mol Plant Microbe Interact* **24**: 1345–1358
- Imazumi-Anraku H, Kouchi H, Syono K, Akao S, Kawaguchi M (2000) Analysis of *ENOD40* expression in *alb1*, a symbiotic mutant of *Lotus japonicus* that forms empty nodules with incompletely developed nodule vascular bundles. *Mol Gen Genet* **264**: 402–410
- Kuppusamy KT, Endre G, Prabhu R, Penmetsa RV, Veereshlingam H, Cook DR, Dickstein R, Vandenbosch KA (2004) *LIN*, a *Medicago truncatula* gene required for nodule differentiation and persistence of rhizobial infections. *Plant Physiol* **136**: 3682–3691
- Lancelle SA, Torrey JG (1985) Early development of Rhizobium-induced root nodules of *Parasponia rigida*. II. Nodule morphogenesis and symbiotic development. *Can J Bot* **63**: 25–35
- Laplaze L, Duhoux E, Franche C, Frutz T, Svistoonoff S, Bisseling T, Bogusz D, Pawlowski K (2000) *Casuarina glauca* pre-nodule cells display the same differentiation as the corresponding nodule cells. *Mol Plant Microbe Interact* **13**: 107–112
- Leigh JA, Signer ER, Walker GC (1985) Exopolysaccharide-deficient mutants of *Rhizobium meliloti* that form ineffective nodules. *Proc Natl Acad Sci USA* **82**: 6231–6235
- Limpens E, Franken C, Smit P, Willemsse J, Bisseling T, Geurts R (2003) LysM domain receptor kinases regulating rhizobial Nod factor-induced infection. *Science* **302**: 630–633
- Lohar DP, Sharopova N, Endre G, Peñuela S, Samac D, Town C, Silverstein KA, VandenBosch KA (2006) Transcript analysis of early nodulation events in *Medicago truncatula*. *Plant Physiol* **140**: 221–234
- Madsen LH, Tirichine L, Jurkiewicz A, Sullivan JT, Heckmann AB, Bek AS, Ronson CW, James EK, Stougaard J (2010) The molecular network



- governing nodule organogenesis and infection in the model legume *Lotus japonicus*. *Nat Commun* **1**: 1–12
- Marie C, Barny MA, Downie JA (1992) *Rhizobium leguminosarum* has two glucosamine synthases, GlmS and NodM, required for nodulation and development of nitrogen-fixing nodules. *Mol Microbiol* **6**: 843–851
- Marsh JF, Rakocevic A, Mitra RM, Brocard L, Sun J, Eschstruth A, Long SR, Schultze M, Ratet P, Oldroyd GED (2007) *Medicago truncatula* NIN is essential for rhizobial-independent nodule organogenesis induced by autoactive calcium/calmodulin-dependent protein kinase. *Plant Physiol* **144**: 324–335
- Mathesius U, Schlaman HR, Spaik HP, Of Sautter C, Rolfe BG, Djordjevic MA (1998) Auxin transport inhibition precedes root nodule formation in white clover roots and is regulated by flavonoids and derivatives of chitin oligosaccharides. *Plant J* **14**: 23–34
- Murray JD (2011) Invasion by invitation: rhizobial infection in legumes. *Mol Plant Microbe Interact* **24**: 631–639
- Murray JD, Karas BJ, Sato S, Tabata S, Amyot L, Szczyglowski K (2007) A cytokinin perception mutant colonized by *Rhizobium* in the absence of nodule organogenesis. *Science* **315**: 101–104
- Murray JD, Muni RRD, Torres-Jerez I, Tang Y, Allen S, Andriankaja M, Li G, Laxmi A, Cheng X, Wen J, et al (2011) *Vapyrin*, a gene essential for intracellular progression of arbuscular mycorrhizal symbiosis, is also essential for infection by rhizobia in the nodule symbiosis of *Medicago truncatula*. *Plant J* **65**: 244–252
- Oldroyd GED, Downie JA (2008) Coordinating nodule morphogenesis with rhizobial infection in legumes. *Annu Rev Plant Biol* **59**: 519–546
- Oldroyd GED, Murray JD, Poole PS, Downie JA (2011) The rules of engagement in the legume-rhizobial symbiosis. *Annu Rev Genet* **45**: 119–144
- Ovchinnikova E, Journet EP, Chabaud M, Cosson V, Ratet P, Duc G, Fedorova E, Liu W, den Camp RO, Zhukov V, et al (2011) IPD3 controls the formation of nitrogen-fixing symbiosomes in pea and *Medicago* Spp. *Mol Plant Microbe Interact* **24**: 1333–1344
- Pacios-Bras C, Schlaman HR, Boot K, Admiraal P, Langerak JM, Stougaard J, Spaik HP (2003) Auxin distribution in *Lotus japonicus* during root nodule development. *Plant Mol Biol* **52**: 1169–1180
- Pichon M, Journet EP, de Billy F, Dedieu A, Huguet T, Truchet G, Barker DG (1994) *ENOD12* gene expression as a molecular marker for comparing rhizobium-dependent and independent nodulation in *Alfalfa*. *Mol Plant Microbe Interact* **7**: 740–747
- Pislaru CI, Murray J, Wen J, Cosson V, Duvvuru Muni RR, Wang M, Benedito V, Andriankaja A, Cheng X, Torres Jerez I, et al (2012) A *Medicago truncatula* tobacco-retrotransposon (Tnt1)-insertion mutant collection with defects in nodule development and symbiotic nitrogen fixation. *Plant Physiol* **159**: 1686–1699
- Plet J, Wasson A, Ariel F, Le Signor C, Baker D, Mathesius U, Crespi M, Frugier F (2011) MtCRE1-dependent cytokinin signaling integrates bacterial and plant cues to coordinate symbiotic nodule organogenesis in *Medicago truncatula*. *Plant J* **65**: 622–633
- Rightmyer AP, Long SR (2011) Pseudonodule formation by wild-type and symbiotic mutant *Medicago truncatula* in response to auxin transport inhibitors. *Mol Plant Microbe Interact* **24**: 1372–1384
- Schauser L, Roussis A, Stiller J, Stougaard J (1999) A plant regulator controlling development of symbiotic root nodules. *Nature* **402**: 191–195
- Sieberer BJ, Chabaud M, Fournier J, Timmers AC, Barker DG (2012) A switch in Ca<sup>2+</sup> spiking signature is concomitant with endosymbiotic microbe entry into cortical root cells of *Medicago truncatula*. *Plant J* **69**: 822–830
- Stacey G, So JS, Roth LE, Lakshmi SK B, Carlson RW (1991) A lipopolysaccharide mutant of *Bradyrhizobium japonicum* that uncouples plant from bacterial differentiation. *Mol Plant Microbe Interact* **4**: 332–340
- Subramanian S, Stacey G, Yu O (2007) Distinct, crucial roles of flavonoids during legume nodulation. *Trends Plant Sci* **12**: 282–285
- Takanashi K, Sugiyama A, Yazaki K (2011) Involvement of auxin distribution in root nodule development of *Lotus japonicus*. *Planta* **234**: 73–81
- Timmers AC, Auriac MC, Truchet G (1999) Refined analysis of early symbiotic steps of the *Rhizobium-Medicago* interaction in relationship with microtubular cytoskeleton rearrangements. *Development* **126**: 3617–3628
- Tirichine L, Imaizumi-Anraku H, Yoshida S, Murakami Y, Madsen LH, Miwa H, Nakagawa T, Sandal N, Albrektsen AS, Kawaguchi M, et al (2006a) Deregulation of a Ca<sup>2+</sup>/calmodulin-dependent kinase leads to spontaneous nodule development. *Nature* **441**: 1153–1156
- Tirichine L, James EK, Sandal N, Stougaard J (2006b) Spontaneous root-nodule formation in the model legume *Lotus japonicus*: a novel class of mutants nodulates in the absence of rhizobia. *Mol Plant Microbe Interact* **19**: 373–382
- Tirichine L, Sandal N, Madsen LH, Radutoiu S, Albrektsen AS, Sato S, Asamizu E, Tabata S, Stougaard J (2007) A gain-of-function mutation in a cytokinin receptor triggers spontaneous root nodule organogenesis. *Science* **315**: 104–107
- Trinick MJ (1979) Structure of nitrogen-fixing nodules formed by *Rhizobium* on roots of *Parasponia andersonii* Planch. *Can J Microbiol* **25**: 565–578
- Truchet G, Roche P, Lerouge P, Vasse J, Camut S, de Billy F, Prome JC, Denarie J (1991) Sulphated lipo-oligosaccharide signals of *Rhizobium meliloti* elicit root nodule organogenesis in alfalfa. *Nature* **351**: 670–673
- Van De Wiel C, Norris JH, Bochenek B, Dickstein R, Bisseling T, Hirsch AM (1990) Nodulin gene expression and ENOD2 localization in effective, nitrogen-fixing and ineffective, bacteria-free nodules of alfalfa. *Plant Cell* **2**: 1009–1017
- Vernié T, Moreau S, de Billy F, Plet J, Combiér JP, Rogers C, Oldroyd G, Frugier F, Niebel A, Gamas P (2008) EFD Is an ERF transcription factor involved in the control of nodule number and differentiation in *Medicago truncatula*. *Plant Cell* **20**: 2696–2713
- Vernoud V, Journet EP, Barker DG (1999) MtENOD20, a Nod Factor-inducible molecular marker for root cortical cell activation. *Mol Plant Microbe Interact* **12**: 604–614
- Voroshilova VA, Demchenko KN, Brewin NJ, Borisov AY, Tikhonovich IA (2009) Initiation of a legume nodule with an indeterminate meristem involves proliferating host cells that harbour infection threads. *New Phytol* **181**: 913–923
- Wasson AP, Pellerone FI, Mathesius U (2006) Silencing the flavonoid pathway in *Medicago truncatula* inhibits root nodule formation and prevents auxin transport regulation by rhizobia. *Plant Cell* **18**: 1617–1629
- Wu C, Dickstein R, Cary AJ, Norris JH (1996) The Auxin Transport Inhibitor *N*-(1-naphthyl)phthalamic acid elicits pseudonodules on non-nodulating mutants of white sweetclover. *Plant Physiol* **110**: 501–510
- Yang C, Signer ER, Hirsch AM (1992) Nodules initiated by *Rhizobium meliloti* exopolysaccharide mutants lack a discrete, persistent nodule meristem. *Plant Physiol* **98**: 143–151
- Zhang J, Subramanian S, Stacey G, Yu O (2009) Flavones and flavonols play distinct critical roles during nodulation of *Medicago truncatula* by *Sinorhizobium meliloti*. *Plant J* **57**: 171–183
- Zhao Z, Andersen SU, Ljung K, Dolezal K, Miotk A, Schultheiss SJ, Lohmann JU (2010) Hormonal control of the shoot stem-cell niche. *Nature* **465**: 1089–1092